ESC European Society of Cardiology
Cardiovascular Research
doi:10.1093/cvr/cvz057

Toll-like receptor 7 deficiency promotes survival and reduces adverse left ventricular remodelling after myocardial infarction

Dominique P.V. de Kleijn[1,2,3,4†‡], Suet Yen Chong[1,2†], Xiaoyuan Wang[1,2†], Siti Maryam J.M. Yatim[1,2], Anna-Marie Fairhurst[5], Flora Vernooij[1], Olga Zharkova[1,2], Mark Y. Chan[2,6], Roger S.Y. Foo[2,7], Leo Timmers[8], Carolyn S.P. Lam[9,10‡], and Jiong-Wei Wang[1,2,11*‡]

[1]Department of Surgery, Yong Loo Lin School of Medicine, National University of Singapore, Singapore, Singapore; [2]Cardiovascular Research Institute (CVRI), National University Heart Centre Singapore (NUHCS), Singapore, Singapore; [3]Netherlands Heart Institute, Utrecht, The Netherlands; [4]Department of Vascular Surgery, University Medical Center Utrecht, Utrecht, The Netherlands; [5]Singapore Immunology Network (SIgN), A*STAR Research Entities, Singapore, Singapore; [6]Department of Medicine, Yong Loo Lin School of Medicine, National University Heart Centre Singapore (NUHCS), Singapore, Singapore; [7]Genome Institute of Singapore, Agency for Science, Technology and Research, Singapore, Singapore; [8]Department of Cardiology, University Medical Center Utrecht, Utrecht, The Netherlands; [9]National Heart Centre Singapore (NHCS), Duke-NUS Graduate Medical School, Singapore, Singapore; [10]Department of Cardiology, University Medical Center, Groningen, The Netherlands; and [11]Department of Physiology, Yong Loo Lin School of Medicine, National University of Singapore, Singapore, Singapore

Received 29 January 2019; revised 18 February 2019; editorial decision 25 February 2019; accepted 28 February 2019

Time for primary review: 19 days

Aims The Toll-like receptor 7 (TLR7) is an intracellular innate immune receptor activated by nucleic acids shed from dying cells leading to activation of the innate immune system. Since innate immune system activation is involved in the response to myocardial infarction (MI), this study aims to identify if TLR7 is involved in post-MI ischaemic injury and adverse remodelling after MI.

Methods and results TLR7 involvement in MI was investigated in human tissue from patients with ischaemic heart failure, as well as in a mouse model of permanent left anterior descending artery occlusion in C57BL/6J wild type and TLR7 deficient ($TLR7^{-/-}$) mice. TLR7 expression was up-regulated in human and mouse ischaemic myocardium after MI. Compared to wild type mice, $TLR7^{-/-}$ mice had less acute cardiac rupture associated with blunted activation of matrix metalloproteinase 2, increased expression of tissue inhibitor of metalloproteinase 1, recruitment of more myofibroblasts, and the formation of a myocardial scar with higher collagen fibre density. Furthermore, inflammatory cell influx and inflammatory cytokine expression post-MI were reduced in the $TLR7^{-/-}$ heart. During a 28-day follow-up after MI, TLR7 deficiency resulted in less chronic adverse left ventricular remodelling and better cardiac function. Bone marrow (BM) transplantation experiments showed that TLR7 deficiency in BM-derived cells preserved cardiac function after MI.

Conclusions In acute MI, TLR7 mediates the response to acute cardiac injury and chronic remodelling probably via modulation of post-MI scar formation and BM-derived inflammatory infiltration of the myocardium.

Keywords TLR7 • Myocardial infarction • Inflammation • Fibrosis • Left ventricular remodelling

1. Introduction

Myocardial infarction (MI) activates the innate immune system that is needed to recruit leucocytes to clear necrotic cells and initiate myocardial repair. Inflammation, however, often also causes detrimental effects to the heart such as cardiac rupture and adverse ventricular remodelling.[1–3]

Cardiac rupture, a fatal complication that often occurs in the early phase after MI, is the main cause of death in murine MI models,[4,5] and accounts for more than 10% of mortality in post-MI patients.[6]

* Corresponding author. Tel: +65 66011387; fax: +65 67778427, E-mail: surwang@nus.edu.sg

† The first three authors are the co-first authors.

‡ These authors are the co-senior authors.

In preclinical studies following MI, degradation of extracellular matrix (ECM) by activated matrix metalloproteinases (MMPs) following MI reduces tissue tension and eventually makes the infarcted heart vulnerable to haemodynamic stress and prone to rupture.[4] This is counterbalanced by proliferation and differentiation of cardiac fibroblasts into myofibroblasts that produce fibrogenic contents including collagens, fibronectin, and periostin to form a provisional ECM replacing granular tissue.[7,8] The balance between ECM degradation and cardiac wound healing dictates cardiac rupture events.

Left ventricular (LV) remodelling after MI is a chronic process including infarct expansion, progressive wall thinning, chamber dilation, and eventually congestive heart failure.[3,9] Given the advanced reperfusion strategies along with modern pharmacological treatments such as β-blockers and angiotensin converting enzyme (ACE) inhibitors, survival after acute MI has been largely improved in last three decades. However, the incidence of congestive heart failure due to adverse LV remodelling in the patients after MI remains high.[10]

Toll-like receptors (TLRs) are innate pathogen recognition receptors that recognize exogenous microorganisms including bacteria and viruses via Pathogen Associated Molecular Patterns (PAMPs) thereby protecting the host from infection.[1–3] They also detect endogenous proteins, DNA and RNA released from dying cells, termed Danger Associated Molecular Patterns (DAMPs).[11] Activation of TLRs results in an inflammatory response leading to the release of cytokines and chemokines and an influx of inflammatory cells.[1–3,11] Following MI, activation of TLR2 and TLR4 in the heart has been shown to exaggerate myocardial injury by recruiting inflammatory cells and increased expression of cytokines and chemokines.[1,12,13] The ECM protein fibronectin-EDA (EIIIA; EDA) is up-regulated after MI and thought to be an endogenous ligand of TLR2 and TLR4.[14] Ablation of EDA prevents cardiac rupture and attenuates cardiac dysfunction in a murine MI model.[14] Distinct from TLR2 and TLR4 that locate on the cell membrane, TLR3, TLR7, and TLR9 are expressed in intracellular compartments such as endosomes and are activated by exogenous (viral or bacterial) or endogenous nuclear acids.[15] Activation of TLR3 by dsRNA released from injured cardiac cells promotes autophagy and exacerbates LV remodelling after MI.[16] In contrast, activation of TLR9, a receptor for DNA rich in CpG motifs, prevents cardiac rupture by promoting myofibroblast proliferation and activation.[17] Whether TLR7 plays a role in the response of the heart to MI is unknown.

TLR7 detection of endogenous ssRNA mediates autoimmune responses in the autoimmune disease systemic lupus erythematosus (SLE).[18,19] Given the opposing inflammatory roles of TLR7 and TLR9 in murine models of SLE,[20,21] the cardiac protective effect of TLR9 in MI,[17] and the observation of elevated levels of circulating extracellular RNAs after acute MI in human and preclinical animal models[22–24] which can activate the TLR7-MyD88 pathway,[25] we hypothesized that TLR7 may be activated after MI resulting in detrimental activation of the innate immune system.

We therefore aimed to investigate whether TLR7 is involved in the cardiac response to acute ischaemic injury and the extent to which it contributes to ventricular repair and adverse remodelling following MI.

2. Methods

2.1 Ethics approval

Human tissue was obtained from the Papworth Hospital (Cambridge) Tissue Bank with an approval by the Cambridgeshire Research Ethics Committee (UK), and from the UK Human Tissue Bank (de Montfort University, UK) with written informed consent obtained for all tissue samples.[26] The study was approved by the Institutional Review Board of National University of Singapore and in compliance with the Declaration of Helsinki.

All mice (10–12 weeks old; 20–25 g) used for this study were of C57BL/6J background. Animals were maintained under a 12/12-h light–dark cycle (lights on at 7 AM, lights off at 7 PM) at the Comparative Medicine Animal Vivarium at National University of Singapore. Mice were maintained in the individually ventilated cages (IVC) with filter tops and received standard diet and water *ad libitum*. Mice were anaesthetized by one i.p. injection of a mixture of 0.5 mg/kg medetomidine, 5.0 mg/kg Dormicum, and 0.05 mg/kg fentanyl. After surgery, animals were recovered by a subcutaneous injection of 0.5 mg/kg atipamezole and 5 mg/kg flumazenil, and received 0.1 mg/kg buprenorphine subcutaneously bid for 3 days. Animals were euthanized with overdose ketamine (225 mg/kg) and medetomidine (3 mg/kg) followed by heart extraction. Murine MI model, echocardiography, and bone marrow (BM) transplantation procedures were described previously.[27–29] All experimental procedures were performed with prior approval and in accordance with the protocols and guidelines of the Institutional Animal Care and Use Committee (IACUC), National University of Singapore; and conform to the Guidelines on the Care and Use of Animals for Scientific purposes (NACLAR, Singapore, 2004) and the Guide for the Care and Use of Laboratory Animals published by the US National Institutes of Health (NIH Publication, 8th Edition, 2011).

2.2 Statistical analysis

Data were analysed with SPSS software (IBM® SPSS® Statistics version 22.0, Armonk, New York, USA). Values are reported as mean ± SEM. Gaussian distribution was assessed and the appropriate Student's *t*-test or Mann–Whitney *U* test was used to compare two groups, with one-way ANOVA followed by Bonferroni *post hoc* test to compare more than two groups. Two-way repeated measures ANOVA was used for comparisons between groups over time. Sample sizes were described in the figure legends. *P*-values ≤ 0.05 were considered statistically significant.

Detailed methods are provided in the Supplementary material online. All the data and materials (including primers for qPCR in Supplementary material online, *Table S1*) supporting the findings of this study are provided within the manuscript and its Supplementary material online, or otherwise available upon reasonable request from the corresponding author.

3. Results

3.1 TLR7 is up-regulated in MI

TLR7 mRNA expression in murine myocardial tissue was detected at a very low level (*Figure 1A*) at baseline (before MI). Immunohistochemical staining of mouse heart tissue showed no detectable TLR7 protein in SHAM-operated hearts (*Figure 1B*). Following MI, myocardial TLR7 mRNA expression was markedly up-regulated at 3 days and increased further at 7 days post-MI (*Figure 1C*). TLR7 positive cells were detected by immunohistochemistry in the remote zone of MI hearts (Supplementary material online, *Figure S1*). Abundant TLR7 positive infiltrates were observed in the infarct and border zones of wild type (WT) hearts at 3 and 7 days post-MI (*Figure 1D* and Supplementary material online, *Figure S1*). As expected, TLR7 was not detected either by qPCR (*Figure 1A*) or by immunohistochemistry (Supplementary material online, *Figure S1*) in TLR7 deficient ($TLR7^{-/-}$) hearts.

Table 1 Echocardiography characterization of WT and TLR7$^{-/-}$ mice

	WT			TLR7$^{-/-}$		
	Baseline	7 days MI	28 days MI	Baseline	7 days MI	28 days MI
HR (b.p.m.)	398 ± 8	442 ± 11**	426 ± 13*	420 ± 10	468 ± 10***	435 ± 13
ESV (μL)	31.4 ± 2.1	92.3 ± 10.1***	112.2 ± 11.4***	33.2 ± 1.8	64.7 ± 3.1***	80.5 ± 5.6***‡
EDV (μL)	66.5 ± 3.0	120.0 ± 9.9***	142.7 ± 11.0***	73.0 ± 2.9	98.7 ± 4.3***	119.8 ± 6.6***
EF (%)	53.6 ± 1.8	26.2 ± 2.6***	23.7 ± 2.2***	54.6 ± 1.7	34.6 ± 0.8***‡	33.9 ± 1.5***¶
FS (%)	27.4 ± 1.3	10.9 ± 1.2***	10.0 ± 1.1***	30.1 ± 1.4	17.5 ± 0.9***§	16.7 ± 0.9***§
CO (mL/min)	14.08 ± 0.71	12.19 ± 0.97*	12.97 ± 1.09	16.61 ± 0.84	15.83 ± 0.71¶	16.98 ± 0.88¶
LVIDs (mm)	2.98 ± 0.09	4.60 ± 0.21***	5.04 ± 0.21***	2.93 ± 0.08	3.99 ± 0.11***‡	4.35 ± 0.14***
LVIDd (mm)	4.08 ± 0.07	5.13 ± 0.17***	5.57 ± 0.17***	4.17 ± 0.06	4.82 ± 0.10***	5.20 ± 0.13***

Echocardiography was performed on the mice at baseline (before MI) and at the indicated time after MI. Paired *t*-test compared to respective baseline, * $P < 0.05$, ** $P < 0.01$, *** $P < 0.001$; Mann–Whitney *U* test compared to WT: ‡ $P < 0.05$, ¶ $P < 0.01$, § $P < 0.001$.

CO, cardiac output; EDV, end-diastolic volume; EF, ejection fraction; ESV, end-systolic volume; FS, fractional shortening; HR, heart rate (beat per minute); LVIDd, left ventricular internal diameter end diastole; LVIDs, left ventricular internal diameter end systole.

To evaluate the pathophysiology and clinical relevance in human ischaemic heart disease, we analysed TLR7 expression in human heart biopsies (clinical characteristics of studied subjects summarized in Supplementary material online, *Table S2*). TLR7 mRNA expression was only detectable in the heart from patients with heart failure secondary to ischaemic heart disease but not in normal hearts (*Figure 1E*). TLR7 protein expression in the ischaemic human heart was further confirmed by immunohistochemical staining (*Figure 1F–H*). In addition to TLR7-positive infiltrates as observed in the mouse heart within the first week post-MI, TLR7-positive cardiomyocytes were present in the ischaemic human heart (*Figure 1H*). Since all ischaemic human heart tissue was obtained at the end stage of heart failure (long time after the initial MI),[26] we examined TLR7 expression in the ischaemic mouse heart at 28 days post-MI. At this timepoint, TLR7 expression was shown in both cardiac infiltrates and some cardiomyocytes (Supplementary material online, *Figure S2*), similar to the findings observed in the ischaemic human heart tissue.

3.2 TLR7 deficiency prevents ventricular rupture, attenuates ventricular remodelling, and preserves cardiac function after MI

To investigate a possible causal role of TLR7 in the response of the heart to MI, MI was induced in WT mice or TLR7$^{-/-}$ mice. Infarct size was similar in WT and TLR7$^{-/-}$ mice (infarct area/LV, 37.9 ± 4.8% for WT vs. 38.7 ± 4.6%, $P = 1.000$; Supplementary material online, *Figure S3*).

3.2.1 Ventricular rupture

TLR7$^{-/-}$ mice had a significantly better survival than their WT counterparts during 28 days follow-up after MI (*Figure 2A*). Postmortem analysis showed that mortality in WT mice (12 out of 34 mice; 35.3%) was caused by ventricular rupture, as evidenced by the massive accumulation of blood in the chest and a slit in the ventricular wall between 3 and 6 days post-MI (*Figure 2B* and *C*). In contrast, only four TLR7$^{-/-}$ mice died after MI with two mice due to ventricular rupture at Days 6 and 9 post-MI while the other two mice suffered sudden death in the fourth week post-MI without ventricular rupture. Taken together this demonstrates that TLR7$^{-/-}$ mice are protected from post-MI ventricular rupture.

3.2.2 Ventricular remodelling

After a large MI, mice suffer from chronic adverse LV remodelling that includes alteration in LV geometry and loss of cardiac function.[3,9] These were assessed using echocardiography. At baseline, there was no difference between WT and TLR7$^{-/-}$ mice in heart rate, cardiac chamber dimensions and volumes, and cardiac function (*Table 1*). Following MI, WT mice displayed a progressive increase in LV chamber dimensions and LV systolic and diastolic volumes, and a decrease in LV function (LVEF, FS, and CO) during the 28 days follow-up, indicating the incidence of LV dilation and cardiac dysfunction. LV dilation and cardiac dysfunction were attenuated in post-MI TLR7$^{-/-}$ mice compared to WT mice (*Figure 2D–F* and *Table 1*).

3.3 TLR7 deficiency inhibits ECM degradation and promotes post-MI cardiac repair and scar maturation

Having found that ventricular rupture was reduced in TLR7 deficient mice, we investigated myocardial ECM turnover, which has been closely associated with cardiac rupture events and LV remodelling.[3–5,7]

3.3.1 ECM degradation

A larger area of remaining acellular matrix was shown in the infarct zone of the heart from TLR7$^{-/-}$ mice at 3 days post-MI compared to WT mice (*Figure 3A–C*), indicating that cardiac ECM degradation following MI was slowed down by TLR7 deficiency.

To understand if the reduced ECM degradation in TLR7$^{-/-}$ mice is attributed to lower activities of MMPs, we performed zymography (*Figure 3D* and *E*). Three days post-MI, abundant activated MMP9 and marginal activated MMP2 were shown in the infarcted myocardium but at similar levels between WT and TLR7$^{-/-}$ mice. Seven days post-MI, levels of activated MMP9 decreased while levels of activated MMP2 increased in both WT and TLR7$^{-/-}$ hearts. Compared to WT hearts, levels of activated MMP2 were significantly lower in TLR7$^{-/-}$ hearts at 7 days post-MI. Expression of tissue inhibitor of metalloproteinase 1 (TIMP-1), the

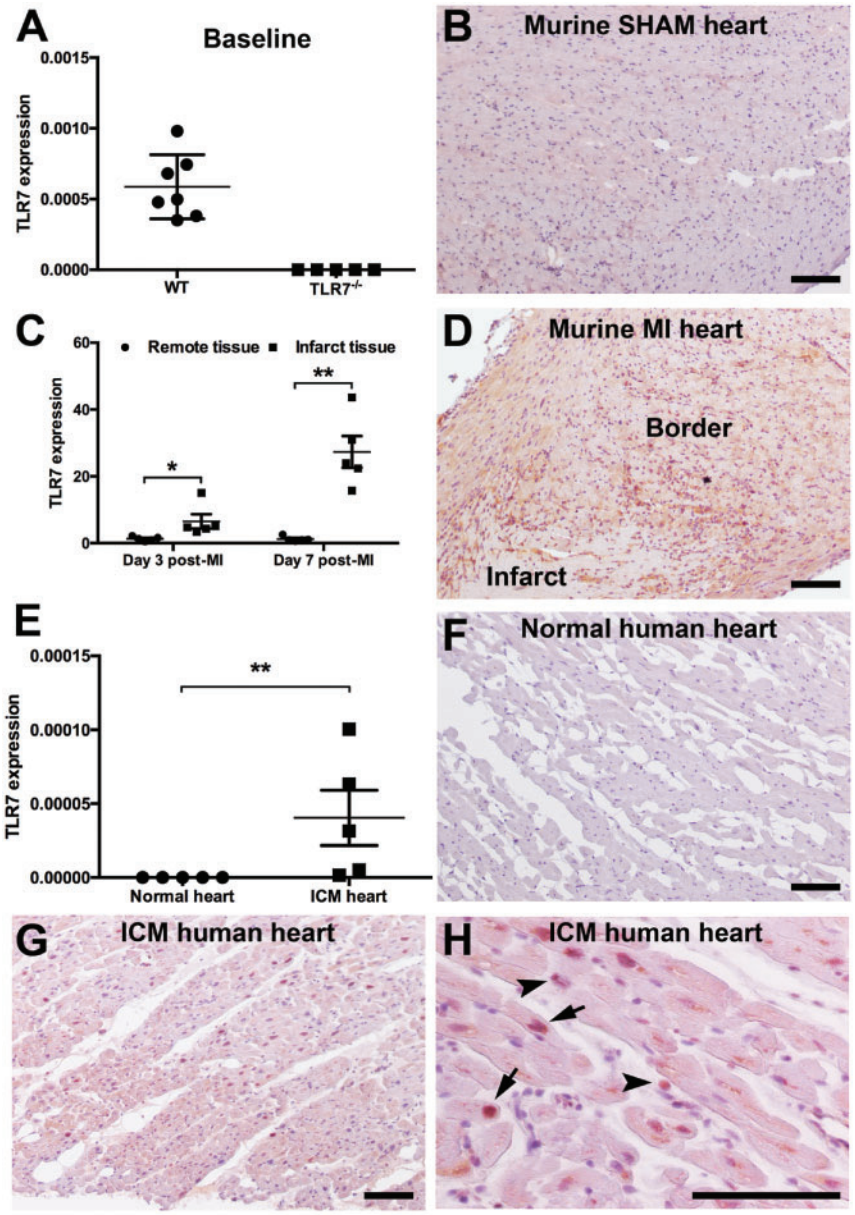

Figure 1 TLR7 expression is up-regulated in ischaemic myocardium in both mice and human. (*A*) Relative expression of TLR7 mRNA in the mouse heart at baseline. Gene expression is normalized to GAPDH. $N = 5–7$ per genotype. (*B*) Immunohistochemical staining of TLR7 in the SHAM heart. No TLR7 staining (indicated in brown) is visible. (*C*) Relative expression of TLR7 mRNA in remote and infarcted heart tissue post-MI. Gene expression is normalized to GAPDH and presented relative to SHAM-operated mice. $N = 5$ per timepoint; Mann–Whitney *U* test, $^{*}P < 0.05$, $^{**}P < 0.01$ compared with WT mice. (*D*) Immunohistochemical staining of TLR7 in a mouse heart at 3 days post-MI. TLR7 staining is indicated in brown. (*E*) Relative expression of TLR7 mRNA in the heart from control subjects ($n = 5$) and heart failure patients ($n = 5$). TLR7 expression is not detectable in control samples. ICM, ischaemic cardiomyopathy. Mann–Whitney *U* test, $^{**}P < 0.01$. (*F*) Representative immunohistochemical staining of TLR7 in a normal heart. No obvious TLR7 staining is observed. (*G, H*) Representative immunohistochemical staining of TLR7 in a failing human heart secondary to ischaemic heart disease. Arrows indicate TLR7 positive cardiomyocytes; arrowheads indicate TLR7 positive infiltrates. Scale bars represent 100 μm.

endogenous inhibitor of MMP2 and 9,[30] was higher in TLR7$^{-/-}$ hearts compared to WT hearts at both 3 and 7 days post-MI (*Figure 3F*). Furthermore, the expression of urokinase type plasminogen activator (uPA)[31] that could activate MMPs via plasminogen[32] was higher in WT hearts at 3 days post-MI (Supplementary material online, *Figure S4A*). In contrast, the expression of plasminogen activator inhibitor-1 (PAI-1) was higher in TLR7$^{-/-}$ hearts (Supplementary material online, *Figure S4B*). These results point to a blunted ECM degradation in TLR7$^{-/-}$ mice.

3.3.2 ECM synthesis

Under MI conditions, ECM synthesis additionally occurs to repair the infarcted heart. The key players for post-MI ECM synthesis including

Table 2 Echocardiography characterization of BM transplanted mice

	Baseline				Post-MI			
	WT/WT BM	WT/TLR7$^{-/-}$ BM	TLR7$^{-/-}$/TLR7$^{-/-}$ BM	TLR7$^{-/-}$/WT BM	WT/WT BM	WT/TLR7$^{-/-}$ BM	TLR7$^{-/-}$/TLR7$^{-/-}$ BM	TLR7$^{-/-}$/WT BM
HR (b.p.m.)	423 ± 10	403 ± 14	434 ± 14	415 ± 16	430 ± 9	413 ± 15	451 ± 27	442 ± 15
ESV (μL)	36.5 ± 1.0	35.6 ± 0.6	36.0 ± 1.5	34.4 ± 0/9	91.1 ± 9.5	54.8 ± 4.5**	58.1 ± 2.6*	72.5 ± 3.6
EDV (μL)	69.7 ± 1.7	69.7 ± 1.5	67.6 ± 2.5	66.7 ± 1.3	114.9 ± 9.3	78.9 ± 5.2**	84.2 ± 4.0	96.2 ± 3.9
EF (%)	47.7 ± 0.4	48.8 ± 0.5	46.8 ± 1.0	48.0 ± 0.3	22.3 ± 1.5	31.3 ± 1.5***	30.9 ± 0.5**	24.8 ± 1.0
FS (%)	24.2 ± 0.5	26.0 ± 0.8	25.5 ± 1.1	26.6 ± 1.1	8.0 ± 0.6	14.7 ± 0.9***	14.1 ± 0.4***	10.3 ± 1.2
CO (mL/min)	14.06 ± 0.50	13.76 ± 0.69	13.80 ± 0.86	13.37 ± 0.50	10.22 ± 0.39	10.01 ± 0.63	11.76 ± 1.10	10.38 ± 0.62
LVIDs (mm)	3.11 ± 0.04	2.99 ± 0.05	3.10 ± 0.09	2.95 ± 0.07	4.94 ± 0.22	3.84 ± 0.12***	4.14 ± 0.08*	4.39 ± 0.15
LVIDd (mm)	4.10 ± 0.04	4.04 ± 0.04	4.15 ± 0.07	4.02 ± 0.05	5.36 ± 0.21	4.50 ± 0.11**	4.82 ± 0.07	4.88 ± 0.12

Echocardiography was performed on the mice at baseline (before MI) and 28 days after MI. One-way ANOVA with Bonferroni *post hoc* tests compared to WT/WT BM mice; *$P < 0.05$; ** $P < 0.01$; *** $P < 0.001$.

CO, cardiac output; EDV, end-diastolic volume; EF, ejection fraction; ESV, end-systolic volume; FS, fractional shortening; HR, heart rate (beat per minute); LVIDd, left ventricular internal diameter end diastole; LVIDs, left ventricular internal diameter end systole.

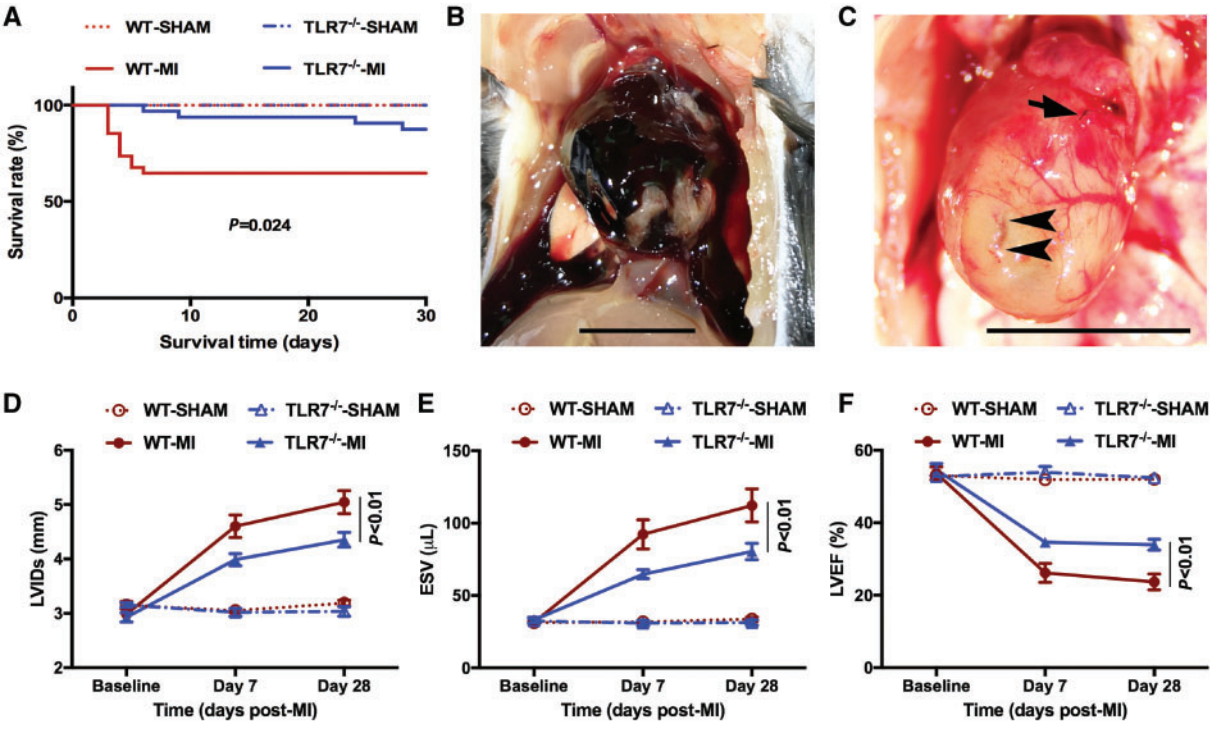

Figure 2 TLR7 deficiency prevents cardiac rupture and ventricular remodelling following MI. (A) The Kaplan–Meier survival curves. Log-rank test, $P = 0.024$; $n = 34$ for WT mice subjected to MI, $n = 31$ for TLR7$^{-/-}$ mice subjected to MI, $n = 10$ for WT SHAM group and $n = 14$ for TLR7$^{-/-}$ SHAM group. (B, C) Representative images of a ruptured heart from a WT mouse died at Day 4 after MI. Scale bars represent 1 cm. Note the blood clots covering the ruptured heart (*B*). After removal of blood clots, the ligation site (indicated by arrow) and a slit (indicated by arrowheads) on the free wall are visible (*C*). (*D–F*) LV chamber dimensions, systolic volumes, and ejection fraction determined by echocardiography. Data were analysed with two-way repeated measures ANOVA. $P < 0.01$ for genotype × time interaction: $F(2, 94) = 6.107$ for LVIDs; $F(2, 94) = 7.945$ for ESV; and $F(2, 94) = 5.292$ for LVEF. $N = 22$ for WT mice and $n = 27$ for TLR7$^{-/-}$ mice subjected to MI, $n = 10$ for WT and $n = 14$ for TLR7$^{-/-}$ SHAM groups. LVIDs, left ventricular internal diameter at end of systole; ESV, end-systolic volume; LVEF, left ventricular ejection fraction.

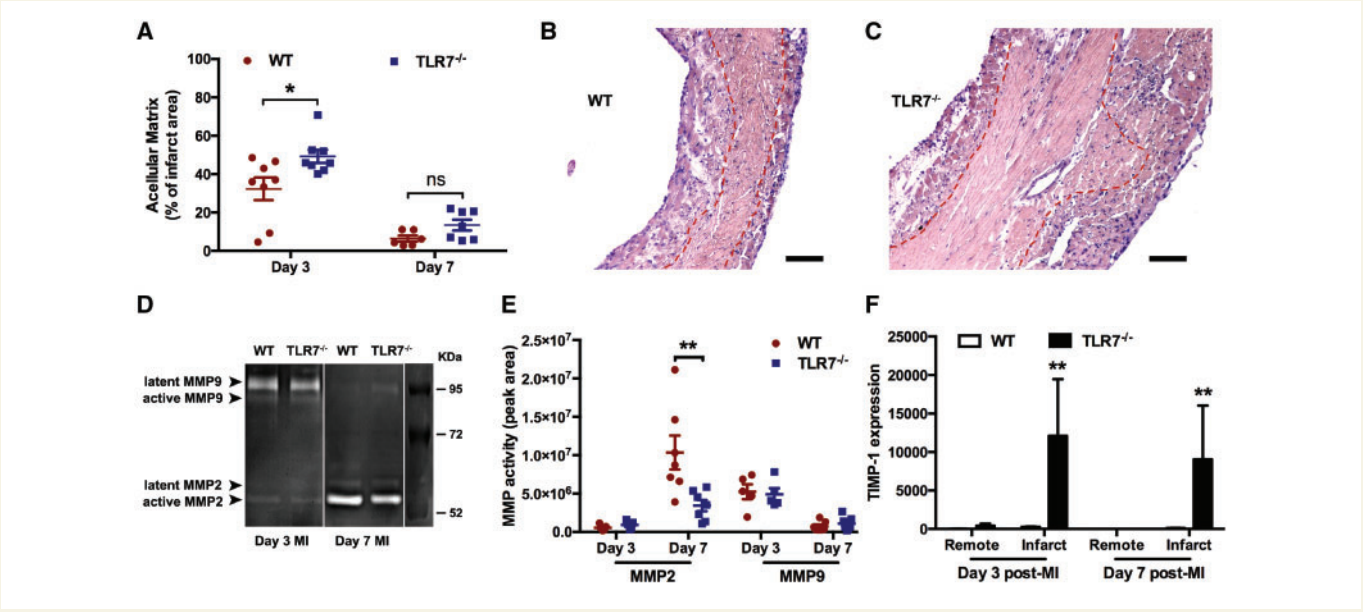

Figure 3 TLR7 deficiency slows down cardiac matrix degradation. (*A*) Area of remaining acellular matrix in the infarct zone during MI development. $N = 6–8$ per timepoint per genotype; Mann–Whitney *U* test, $^{*}P < 0.05$ compared with WT mice; ns, not significant. (*B, C*) Representative H&E staining showing acellular matrix in the post-MI hearts. Red dashed lines demarcate acellular matrix. Scale bars represent 100 μm. (*D*) Representative images of zymography showing expression of MMP2 and MMP9 in the infarcted heart tissue. (*E*) MMP activities quantified by peak areas as described in the Methods section. (*F*) Relative expression of TIMP-1 mRNA in the heart after MI. Gene expression is presented relative to WT SHAM-operated mice. $N = 6–8$ per timepoint per genotype; Mann–Whitney *U* test, $^{**}P < 0.01$ compared with WT mice.

collagen production are alpha-smooth muscle actin (α-SMA) expressing myofibroblasts.[7,33]

We first examined the recruitment of myofibroblasts to the infarcted heart. Cardiac mRNA levels of α-SMA were up-regulated after MI in both WT and TLR7$^{-/-}$ mice at 3 and 7 days (*Figure 4A* and *B*), suggesting an increase in myofibroblasts following MI. Compared to WT mice, expression of α-SMA mRNA in the infarcted myocardium was significantly higher in TLR7$^{-/-}$ mice at 3 days post-MI (*Figure 4A*) followed by more α-SMA positive cells in the infarct zone of TLR7$^{-/-}$ heart at 7 days post-MI (*Figure 4B*).

During cardiac repair, matricellular proteins are pivotal for myofibroblast activation and subsequent infarct healing.[7] We examined the mRNA expression of five matricellular proteins in the infarcted myocardium and found all of them were upregulated in both WT and TLR7$^{-/-}$ mice after MI (*Figure 4C* and Supplementary material online, *Figure S5*). Compared to WT hearts, the expression of periostin was remarkably higher in TLR7$^{-/-}$ hearts at 3 days post-MI (*Figure 4C*), and the expression of thrombospondin 1 and osteopontin were significantly higher at 7 days post-MI (Supplementary material online, *Figure S5*). The expression of osteoglycin and secreted protein acidic and rich in cysteine (SPARC) tended to be higher in TLR7$^{-/-}$ hearts at 7 days post-MI but was not statistically significant (Supplementary material online, *Figure S5*). Given that all those matricellular proteins have been reported to protect post-MI cardiac rupture in mice,[7] the association of higher mRNA levels of those matricellular proteins in TLR7$^{-/-}$ hearts with lesser cardiac rupture suggests that the 'remaining area' observed in *Figure 3* is a bioactive 'acellular matrix'.

TGF-β1, a multifunctional growth factor that is involved in collagen turn-over, also showed higher levels in the infarcted myocardium of TLR7$^{-/-}$ mice at 3 days post-MI (*Figure 4D*). Collagens produced by myofibroblasts are essential to form an organized collagen-based scar in cardiac repair.[7] After MI, expression of alpha-1 type I collagen (Col1a1) was markedly up-regulated in the infarcted myocardium (*Figure 4E*). Compared to WT, higher mRNA levels of Col1a1 were observed in the infarcted myocardium of TLR7$^{-/-}$ mice. Expression of alpha-1 type III collagen (Col3a1) was also increased following MI but showed no difference between WT and TLR7$^{-/-}$ mice (*Figure 4F*). This higher production of collagen 1a1 (*Figure 4E*) together with the lower gelatin degradation (*Figure 3D–F*) in the infarct zone of TLR7$^{-/-}$ heart and denser collagen fibres (*Figure 4G*) in TLR7$^{-/-}$ mice at 28 days post-MI, as shown by Picrosirius Red staining (*Figure 4H* and *I*), shows that collagen turn-over has shifted towards collagen fibre formation.

3.4 TLR7 deficiency reduces cardiac inflammation following MI

Influx of leucocytes into the infarct area is an important inflammatory response to cardiac injury.[1,3] Neutrophil infiltration in the infarct area was high at Day 3 (*Figure 5A*) but no difference was found between TLR7$^{-/-}$ and WT mice. Influx of CD3^{+} T-cells (*Figure 5B*) was lower in the infarct area in TLR7$^{-/-}$ mice at 3 days post-MI in comparison to WT mice. Macrophage influx was lower in TLR7$^{-/-}$ hearts compared to WT hearts in the infarct and border zones at 3 and 7 days as well as in the remote zone at 7 days post-MI (*Figure 5C–F*).

Since influx of inflammatory cells was reduced in TLR7$^{-/-}$ mice, we further investigated if expression of inflammatory cytokines and chemokines was blunted by TLR7 deficiency. As determined by a multiplex assay, protein levels of a broad spectrum of cytokines and chemokines were lower in both remote and infarcted myocardium of TLR7$^{-/-}$ mice (*Figure 6*). At 3 days post-MI, myocardial levels of IL1α, IL2, IL6, IL17,

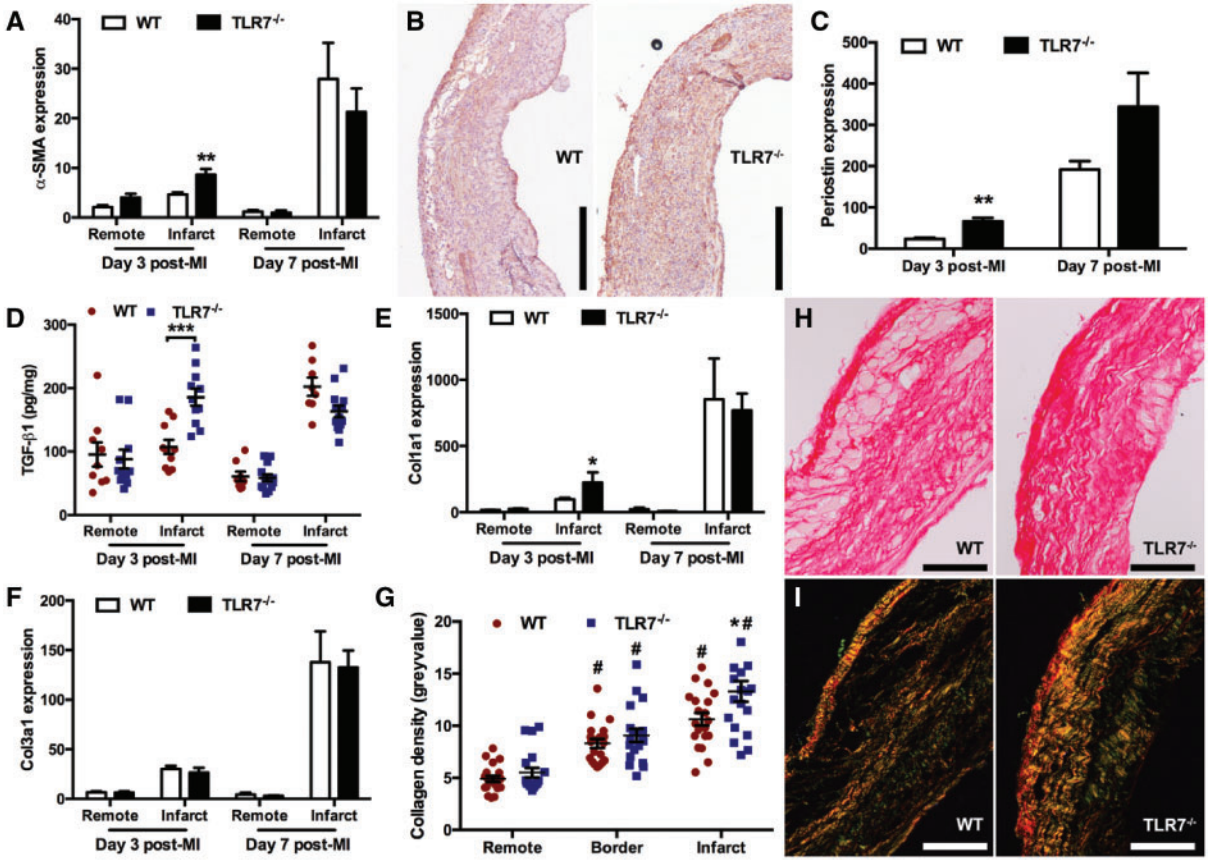

Figure 4 TLR7 deficiency promotes cardiac repair and scar formation. (*A*) Relative expression of α-SMA mRNA in the heart tissue post-MI. Gene expression is presented relative to WT SHAM-operated mice. $N = 6–8$ per timepoint per genotype; Mann–Whitney *U* test, $^{**}P < 0.01$ compared with WT mice. (*B*) Representative staining of α-SMA (in brown) in the infarct zone at 7 days post-MI. Scale bars represent 500 μm. (*C*) Relative expression of periostin mRNA in the infarcted heart tissue post-MI. Gene expression is presented relative to SHAM-operated mice. $N = 5$ per timepoint per genotype; Mann–Whitney *U* test, $^{**}P < 0.01$ compared with WT mice. (*D*) TGFβ1 protein levels in the heart tissue. $N = 8–10$ per timepoint per genotype; Mann–Whitney *U* test, $^{***}P < 0.001$ compared with WT mice. (*E, F*) Relative mRNA expression of Col1a1 and Col3a1 in the heart tissue post-MI. Gene expression is presented relative to WT SHAM-operated mice. $N = 6–8$ per timepoint per genotype; Mann–Whitney *U* test, $^{*}P < 0.05$ compared with WT mice. (*G*) Quantification of collagen content in the scar 28 days post-MI. $N = 20$ for WT mice and $n = 19$ for TLR7$^{-/-}$ mice, Mann–Whitney *U* test, $^{*}P < 0.05$ compared with WT mice; $^{\#}P < 0.05$ compared with remote zone. (*H, I*) Representative infarct sections of WT and TLR7$^{-/-}$ hearts, 28 days post-MI, stained by Picrosirius Red and shown under white light or polarized light (10× magnification). Scale bars represent 100 μm.

RANTES, and TNFα were lower in TLR7$^{-/-}$ mice compared to WT mice, whereas protein level of the anti-inflammatory cytokine MIP1β[34] was higher in TLR7$^{-/-}$ mice (*Figure 6A* and *B*). At 7 days post-MI, GM-CSF, MCP1, MIP1α, and MIP1β were all lower in TLR7$^{-/-}$ mice (*Figure 6C* and *D*).

3.5 TLR7 on BM-derived inflammatory cells mediates MI-induced ventricular adverse remodelling

To investigate whether expression of TLR7 in the heart or in the infiltrating leucocytes determines ventricular remodelling, we generated chimeric mice by BM transplantation: WT/WT BM, TLR7$^{-/-}$/TLR7$^{-/-}$ BM, WT/TLR7$^{-/-}$ BM, and TLR7$^{-/-}$/WT BM (*Figure 7A*). The BM chimera was confirmed by FACS analysis of TLR7 expression in circulating immune cells after a 6-week BM reconstitution (Supplementary material online, *Figure S6A*). The post-MI survival rates were similar among all the groups with only 1 WT/WT BM mouse died of post-MI cardiac rupture during the 28-day follow-up (Supplementary material online, *Figure S6B*). The infarct size, estimated by echocardiography at 28 days post-MI, did not differ among the four chimeric groups (Supplementary material online, *Figure S6C* and *D*). At baseline, there was no difference in echocardiographic parameters among the four chimeric groups (*Table 2*). At 28 days after MI, similar to the complete TLR7$^{-/-}$ and complete WT mice without BM transplantation (*Figure 2*), LV chamber dilation, and LVEF decrease were less severe in TLR7$^{-/-}$/TLR7$^{-/-}$ BM mice compared to WT/WT BM mice (*Table 2* and *Figure 7B* and *C*). WT mice receiving TLR7$^{-/-}$ BM had a better preservation of LV geometry (LV volumes and chamber dimensions) and cardiac function (LVEF and LVFS) compared to those receiving WT BM comparable to TLR7$^{-/-}$ mice receiving TLR7$^{-/-}$ BM. These results show that BM-derived TLR7 determines post-MI LV remodelling.

To further elucidate the cellular source of TLR7, we analysed TLR7 expression and its activation in isolated cardiomyocytes, cardiac

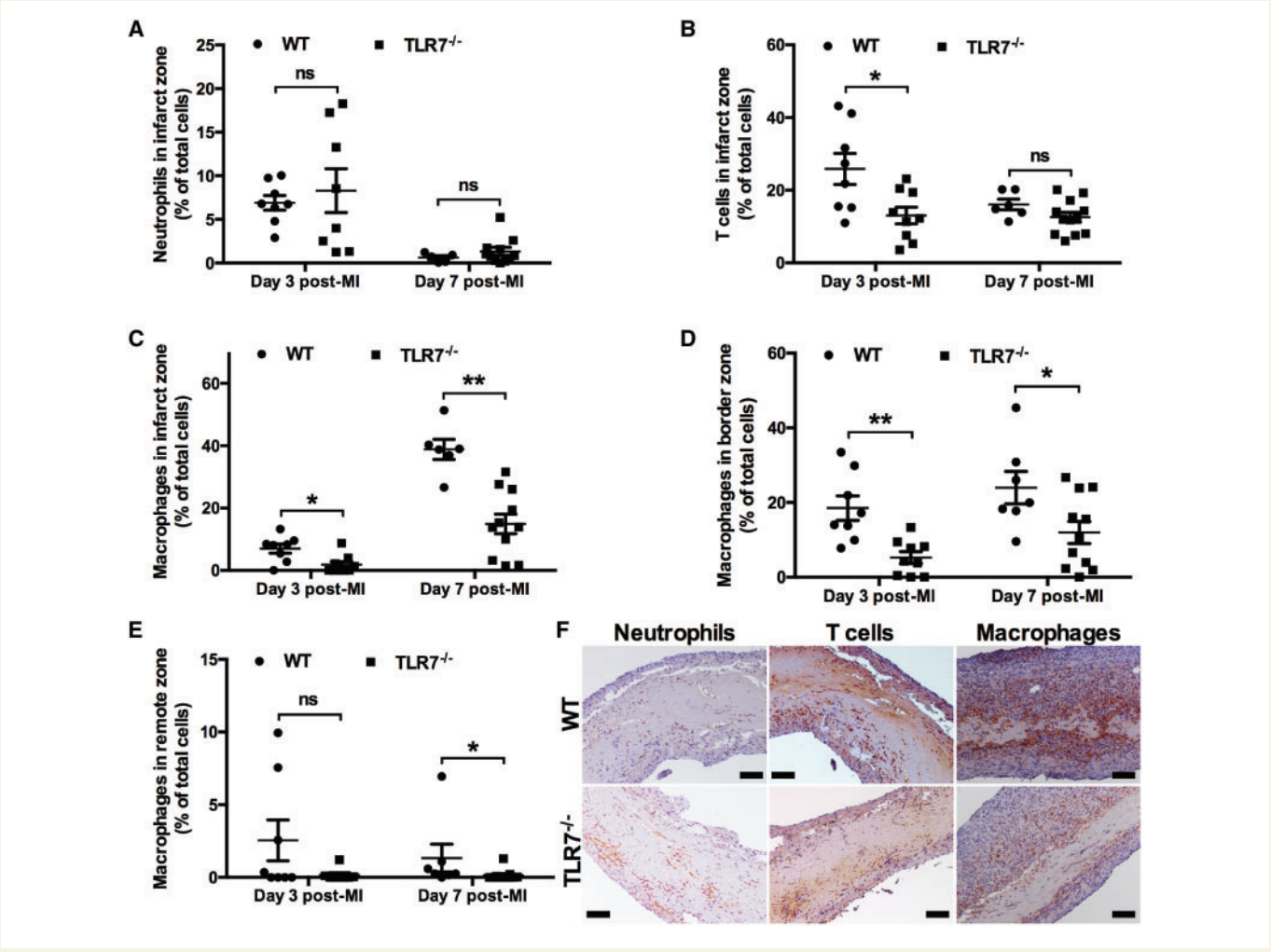

Figure 5 Influx of inflammatory cells into myocardium. (*A–E*) Infiltrated neutrophils, T cells, and macrophages were quantified in the MI hearts. $N = 6–8$ per timepoint per genotype; Mann–Whitney *U* test, $^{*}P < 0.05$, $^{**}P < 0.01$ compared with WT mice. ns, not significant; F, representative infarct sections stained for neutrophils, T cells, and macrophages (10× magnification). Scale bars represent 100 μm.

fibroblasts, and BM-derived macrophages from adult mice. As shown in Supplementary material online, *Figure S7*, TLR7 was highly expressed in macrophages but not detectable in cardiomyocytes or cardiac fibroblasts. In contrast to TLR7$^{-/-}$ macrophages, WT macrophages were activated (loss of CD115 expression) and obtained a proinflammatory phenotype (increased expression of CD38, IL1β, and TNFα) upon exposure to a TLR7 agonist, R848 (Supplementary material online, *Figure S8*). Furthermore, a wide range of cytokines and chemokines were secreted from those macrophages in response to R848 stimulation (Supplementary material online, *Table S3*). No response to R848 was observed in cardiomyocytes or fibroblasts.

4. Discussion

Inflammation is a key mechanism driving cardiac repair and remodelling after MI. In this study, we found that TLR7 expression levels in cardiac tissue were increased in both the murine MI model and patients with ischaemic heart failure. Genetically deficient TLR7 mice showed less frequent post-MI cardiac rupture and less adverse LV remodelling, probably due to enhanced cardiac repair and scar formation, as well as attenuated myocardial inflammation. We also showed that TLR7 in the BM-derived leucocytes is a key component in driving the inflammatory events following MI. These findings unveiled a causal pathophysiological role of TLR7 in the setting of MI, as illustrated in *Figure 8*.

Several lines of evidence point to a direct involvement of TLR7 in cardiovascular disease. Previous data have shown that TLR7 can mediate autoimmune responses via detection of endogenous ssRNA immune-complexes in SLE. These patients have between 5 and 10 times higher risk of acute MI at a young age than their peers within the general population.[18,19,35,36] This may reflect in such patients a generally activated inflammatory state that constitutes a risk factor for cardiovascular disease. In line with this, TLR7-positive macrophages were observed in the hearts of patients with congenital heart block but not in the hearts of healthy donors.[37,38] TLR7 exaggerates atherosclerosis in ApoE deficient mice fed with high fat diet.[39,40] Furthermore, TLR7 mediates inflammation in experimental autoimmune myocarditis and virus-induced myocarditis in mice.[41] We now show for the first time that TLR7 is causally involved in

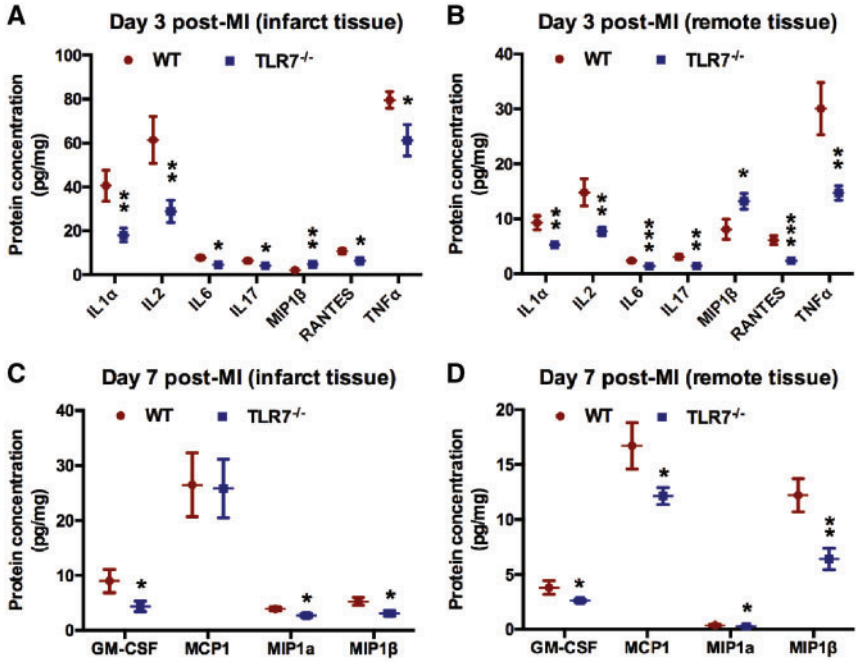

Figure 6 Production of cytokines and chemokines. Protein concentrations of cytokines and chemokines in tissue lysates were quantified by multiplex assays at different timepoints post-MI. $N = 8–10$ per timepoint per genotype; Mann–Whitney U test, $^{*}P < 0.05$, $^{**}P < 0.01$, and $^{***}P < 0.001$ compared with WT mice.

cardiac injury and plays a detrimental role in cardiac repair and LV remodelling following MI.

Cardiac rupture, a catastrophic complication following MI, typically leads to 30–50% mortality for C57BL/6 mice within 7 days after MI.[4] Consistent with prior reports, a moderate infarct size (38% of LV) resulted in 35% of rupture frequency in WT mice in our study. Strikingly, TLR7 deficiency delayed and reduced cardiac rupture events from 35.3% (WT mice) to 6.5% (TLR7$^{-/-}$ mice) during the 28-day follow-up after MI. Since our experimental animals were gender and age matched, and the infarct size and heart rates between WT and TLR7$^{-/-}$ mice were similar, we conclude that the differential rupture frequency was attributed to TLR7. Similar rupture-preventive effects have been reported for ablation of TLR3, EDA (an endogenous ligand of TLR2 and TLR4), and a newly identified nuclear-sensor cyclic GMP-AMP synthase (cGAS) among others.[7,14,31,42–44]

Mechanistically, cardiac rupture is associated with ECM turnover and inflammation severity.[3,4,7,44] We examined the activities of MMP2 and MMP9, two gelatin degrading enzymes that have been closely associated with cardiac rupture after MI.[31,43,44] Although MMP9 activity after MI increased as previously reported[44] but was not different between WT and TLR7$^{-/-}$ mice, we found that MMP2 activity in the infarcted myocardium was significantly lower in TLR7$^{-/-}$ mice. In addition, the mRNA levels of TIMP-1 in infarcted WT hearts (*Figure 3F*) and in TLR7 activated WT macrophages (Supplementary material online, *Figure S9A*) were lower compared to TLR7$^{-/-}$ hearts and macrophages, respectively. These lower MMP2 levels together with the high expression of TIMP-1 in TLR7$^{-/-}$ mice strongly suggest reduced collagen breakdown. Indeed, inhibition of MMP2 activity has been shown to prevent post-MI cardiac rupture.[43]

The plasminogen activation system that can activate MMPs has been implicated in post-MI cardiac rupture by showing that ablation of uPA[31] or plasminogen[32] prevented cardiac rupture in MI. In this study, we found lower expression of uPA but higher expression of PAI-1 in the infarcted myocardium in TLR7$^{-/-}$ mice compared to that in WT mice, suggesting a lower activation of plasminogen system in TLR7$^{-/-}$ hearts. Paradoxically, TLR7 activation by its agonist R848 inhibited expression of uPA without affecting PAI-1 in macrophages *in vitro* (Supplementary material online, *Figure S9B* and *C*). The higher expression of uPA in WT hearts after MI is probably due to a higher number of recruited macrophages and other inflammatory cells into WT hearts, whereas the higher expression of PAI-1 in TLR7$^{-/-}$ hearts is likely due to the higher number of myofibroblasts which express much more PAI-1 than macrophages (Supplementary material online, *Figure S9D*). Our results are consistent with Heymans *et al.*[31] in showing that lower uPA in the heart was associated with protection from post-MI cardiac rupture.

We now show a role for TLR7 in regulation of this process, mediated by bone-marrow derived cells. Cardiac rupture is usually associated with higher inflammation in the infarcted myocardium.[3–5,7,14,31,32,42–44] This is in accordance with the lower levels of inflammation (recruitment of inflammatory cells and production of cytokines and chemokines) in the TLR7$^{-/-}$ hearts with a lower cardiac rupture incidence.

In the response to injury, inflammatory cells are also recruited to clear up dying cardiomyocytes and cell debris and secrete cytokines including IL1β and TNFα that can activate MMPs while inhibit TIMP-1 expression, and subsequently degrade cardiac ECM.[2–9,45,46] This is a delicate balance that with a too high inflammatory response may result in cardiac rupture but on the other hand too little inflammation will result in no or delayed wound healing. TLR7 deficiency partly inhibits the post-MI inflammatory

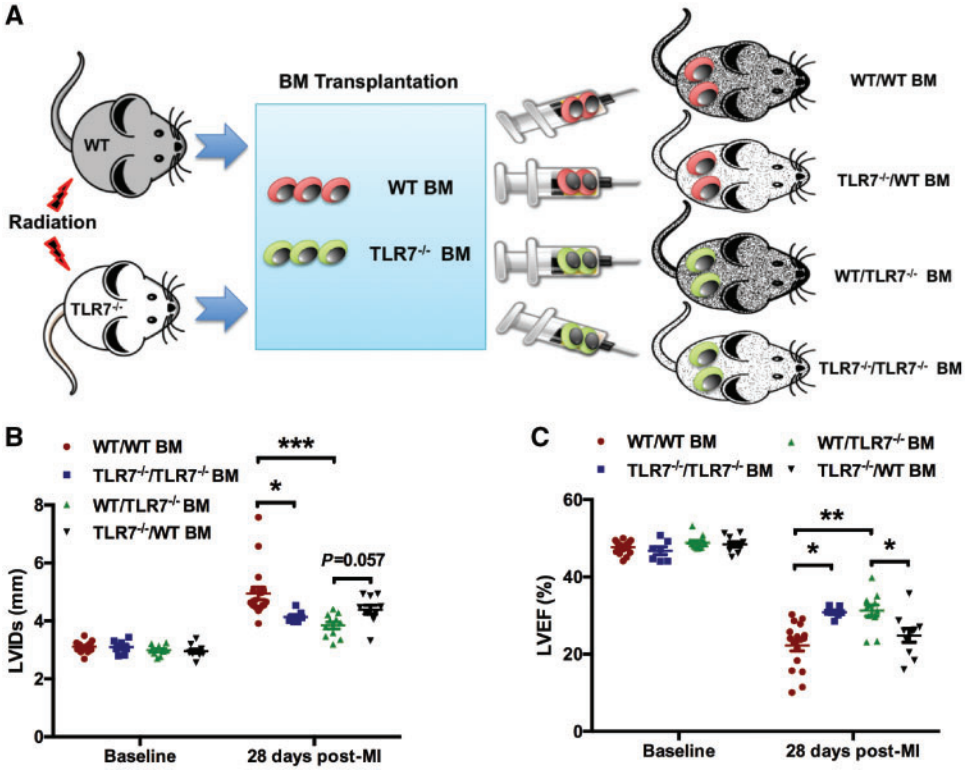

Figure 7 TLR7 expressed in BM-derived cells mediates cardiac dysfunction after MI. (*A*) A schematic diagram illustrating generation of four chimeric groups of mice: WT/WT BM indicates WT mice with WT BM ($n = 17$); TLR7$^{-/-}$/TLR7$^{-/-}$ BM, TLR7$^{-/-}$ mice with TLR7$^{-/-}$ BM ($n = 7$); WT/TLR7$^{-/-}$ BM, WT mice with TLR7$^{-/-}$BM ($n = 11$); TLR7$^{-/-}$/WT BM, TLR7$^{-/-}$ mice with WT BM ($n = 10$). LV systolic chamber dimension (*B*) and ejection fraction (*C*) were determined by echocardiography. One-way ANOVA with Bonferroni *post hoc* tests, *$P < 0.05$, **$P < 0.01$.

response by reducing the influx of TLR7-expressing macrophages. This partial inhibition of inflammatory response slowed down or delayed, as indicated by 'acellular matrix', the clearance of dead cardiomyocytes and degradation of ECM in TLR7$^{-/-}$ mice but did not completely block the processes as seen in the uPA and plasminogen deficient mice.[31,32] This may explain that LV function is protected in TLR7$^{-/-}$ mice. In addition, the increased expression of matricellular proteins such as periostin in TLR7$^{-/-}$ hearts may also contribute to the lesser cardiac rupture and promote the infarct healing by recruiting and activating myofibroblasts.[7] This is in line with the expression of α-SMA suggesting that TLR7 deficiency stimulates recruitment and activation of myofibroblasts following MI. Enrichment of myofibroblasts in TLR7$^{-/-}$ mice increased production of TGFβ and procollagen 1 thereby promoting scar formation in the infarcted heart. Omiya *et al.*[17] recently reported that activation of TLR9 could prevent cardiac rupture by promoting activation of myofibroblasts in the heart after MI. Given the opposing roles of TLR9 and TLR7 in murine SLE[20,21] and atherosclerosis,[40,47] and now also in post-MI cardiac repair, this suggests that TLR7 and TLR9 may share some signalling pathways but counterbalance each other's activation downstream of the signalling pathways.

In humans, the incidence of cardiac rupture has remarkably decreased due to timely reperfusion, whereas the prevalence heart failure has increased in MI survivors due to chronic LV remodelling.[9,10] Nonetheless, cardiac rupture is the penultimate expression of myocardial scar expansion, which is a key determinant of LV ventricular remodelling after MI. A conceptual framework of equilibrium in cardiac fibrosis after severe myocardial injury like ST-segment elevation MI (STEMI) is that fibrosis is sufficiently localized to prevent myocardial scar expansion but yet does not expand beyond the infarct region. LV remodelling following MI is mediated by cardiac inflammation.[2,3,9] Following ischaemic injury, an influx of inflammatory cells into infarcted myocardium results in a robust production of inflammatory cytokines/chemokines and activation of elastase and MMPs, which in turn destroy cardiac ECM leading to cardiac injury and LV remodelling.[2,3,7] In TLR7$^{-/-}$ hearts, post-MI, the influx of inflammatory cells (T cells and macrophages), and the production of proinflammatory cytokines and chemokines were lower compared to WT hearts. However, anti-inflammatory cytokines and chemokines including TGFβ and MIP1β were higher in TLR7$^{-/-}$ hearts.[48] LV remodelling was attenuated as evidenced by preservation of LV volumes and chamber dimensions. In TLR7$^{-/-}$ mice, despite a more mature scar containing more collagen fibres, we did not see an increase in fibrosis in the remote heart tissue, which is consistent with the observed better overall LV function.

TLR7 mRNA has been detected in a variety of cell types including cardiomyocytes and inflammatory cells.[15,25,49] To understand the cellular source of TLR7 that plays a major role in the setting of MI, we generated chimeric mice by BM transplantation. Similar to TLR2 and TLR4,[12,13,29] TLR7 expressed in BM-derived cells rather than resident cardiac cells predominantly mediates post-MI LV remodelling and cardiac

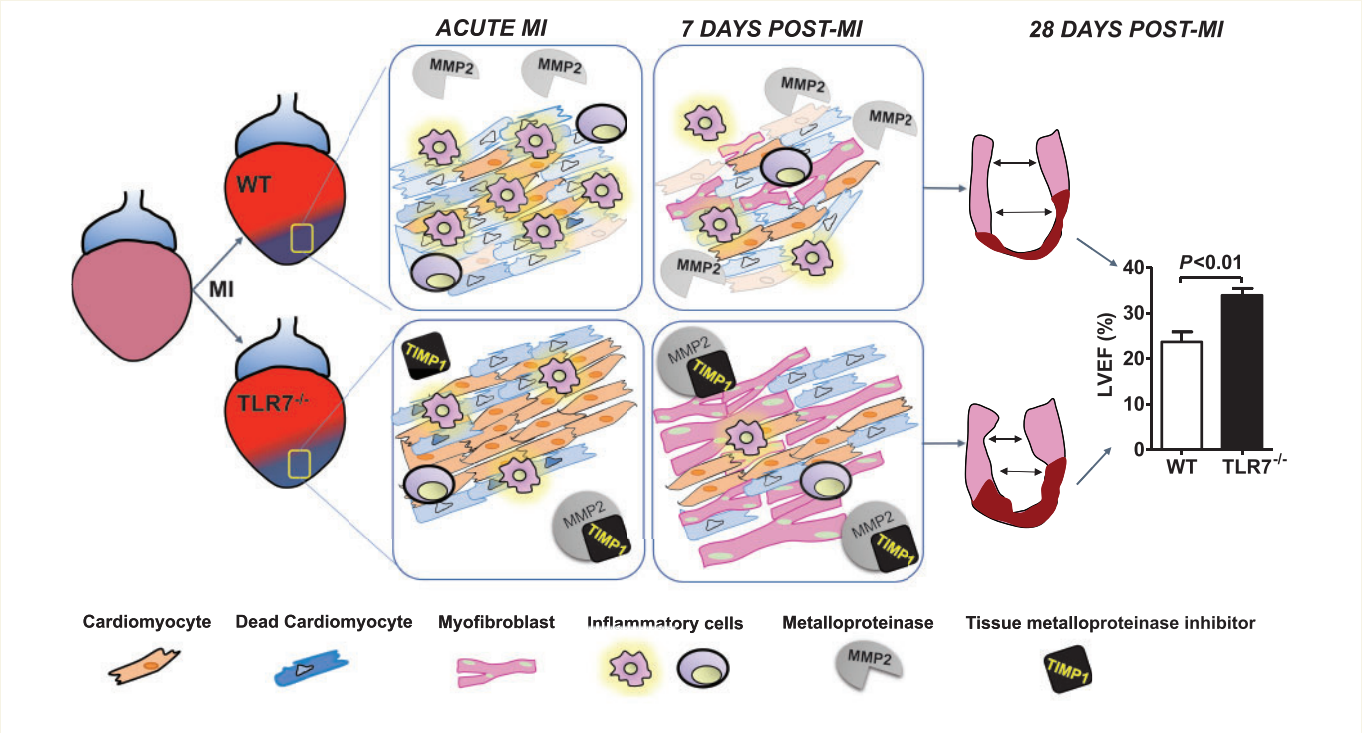

Figure 8 An illustrative summary. Following MI, TLR7 deficiency blunts the cardiac inflammatory responses (cell infiltration and cytokine expression), promotes cardiac repair (lower MMP2 activity, higher TIMP1 expression, and more abundant myofibroblasts), attenuates LV chamber dilation and preserves cardiac function (higher LVEF at 28 days post-MI; Mann–Whitney *U* test).

dysfunction. This is further confirmed by the high expression of TLR7 in BM derived macrophages vs. absence of TLR7 in isolated resident cardiac cells (cardiomyocytes and fibroblasts) as well as their differential response to the TLR7 agonist R848 *in vitro*. In contrast to our isolated adult cardiomyocytes, expression of TLR7 was reported in an immortalized murine cardiomyocyte cell line (HL-1)[49] and rat neonatal cardiomyocytes.[25] This suggests that cardiomyocytes are able to express TLR7 under certain circumstance. In fact, we did find expression of TLR7 in both cardiomyocytes and cardiac infiltrates in human and mice with chronic cardiac ischaemia suggesting that TLR7 also in cardiomyocytes may play a role.[25]

The endogenous ligands of TLR7 in MI, however, remain unclear. We assume that dying cardiac cells will release a large spectrum of 'danger signals', termed as DAMPs, which activate the innate immune system and trigger inflammatory responses for cardiac repair and remodelling.[1–3,11] Cytosolic DNA and RNA released from dying cardiac cells were recently reported to aggravate cardiac injury via activation of 'nuclear sensors' including cyclic GMP-AMP synthase (cGAS), TLR9 and TLR3.[16,17,42] For TLR7, we postulate that extracellular RNAs are released into circulation following MI and modulate cardiac inflammation in mice;[23,24] furthermore the released RNAs may be carried by extracellular vesicles[50] to protect them from RNase degradation. Our postulations arise from the following evidences: first, *in vitro*, extracellular RNAs trigger inflammatory cytokine production partly via TLR7 signalling pathway,[25] and R848 could activate WT macrophages to produce inflammatory cytokines/chemokines but not TLR7$^{-/-}$ macrophages; second, in humans, a major shift in circulating microRNA profile is detectable shortly after acute MI;[22] third, microRNAs carried by extracellular vesicles activate TLR7 and promote prometastatic inflammatory response;[50] fourth, ssRNA circulates in the form of immune-complex and activates TLR7 in SLE.[19] In the setting of MI, the target cells are likely the infiltrated macrophages as the dynamics of TLR7 expression is similar to macrophage infiltration and is in line with our bone-marrow transplantation experiments. This hypothesis is further supported by a recent discovery that cardiac extracellular vesicles are released upon ischaemia injury and taken up by infiltrated monocytes/macrophages thereby regulating cardiac inflammation following MI.[51–53]

To summarize, TLR7 deficient mice showed less cardiac rupture and adverse LV remodelling after MI, probably via improved scar formation and attenuated inflammation. TLR7 expressed in bone-marrow derived cells mediates cardiac inflammation, cardiac repair, and adverse LV remodelling following MI. Our findings identify TLR7 as a potential therapeutic target for post-MI adverse LV remodelling.

Supplementary material

Supplementary material is available at *Cardiovascular Research* online.

Acknowledgements

We thank Dr Ilonka Guenther, Dr Rex Manguiat, and Mr Abdul Malik for their technical assistance of ultrasound and irradiation, Ms Shi Ling Ng and Ms Zenia Tiang for their generous help to arrange human samples, and Ms Hui Yin Lee for her technical assistance of flow cytometry.

Conflict of interest: none declared.

Funding

This work was supported by the National University Health System collaborative grant (NUHS O-CRG 2016 Oct-23) and the Singapore Ministry of Health's National Medical Research Council grant (NMRC/OFYIRG/0081/2018) to J.W.W.; NMRC CS-IRG (CS-IRG13nov024), NMRC Centre Grant, and ATTRaCT SPF grant to C.S.P.L. and D.P.V.d.K.; Start-up grant National University of Singapore, NMRC Star award and KNAW strategic grant to D.P.V.d.K.; Ministry of Education NUSMed Post-Doctoral Fellowship (NUHSRO/2017/074/PDF/04 to J.W.W.) to O.Z.

References

1. Arslan F, de Kleijn DP, Pasterkamp G. Innate immune signaling in cardiac ischemia. *Nat Rev Cardiol* 2011;**8**:292–300.
2. Mann DL. Innate immunity and the failing heart: the cytokine hypothesis revisited. *Circ Res* 2015;**116**:1254–1268.
3. Frangogiannis NG. The inflammatory response in myocardial injury, repair, and remodelling. *Nat Rev Cardiol* 2014;**11**:255–265.
4. Gao XM, Xu Q, Kiriazis H, Dart AM, Du XJ. Mouse model of post-infarct ventricular rupture: time course, strain- and gender-dependency, tensile strength, and histopathology. *Cardiovasc Res* 2005;**65**:469–477.
5. Lindsey ML, Bolli R, Canty JM, Jr., Du XJ, Frangogiannis NG, Frantz S, Gourdie RG, Holmes JW, Jones SP, Kloner RA, Lefer DJ, Liao R, Murphy E, Ping P, Przyklenk K, Recchia FA, Schwartz Longacre L, Ripplinger CM, Van Eyk JE, Heusch G. Guidelines for experimental models of myocardial ischemia and infarction. *Am J Physiol Heart Circ Physiol* 2018;**314**:H812–H838.
6. Pouleur AC, Barkoudah E, Uno H, Skali H, Finn PV, Zelenkofske SL, Belenkov YN, Mareev V, Velazquez EJ, Rouleau JL, Maggioni AP, Kober L, Califf RM, McMurray JJ, Pfeffer MA, Solomon SD, Investigators V. Pathogenesis of sudden unexpected death in a clinical trial of patients with myocardial infarction and left ventricular dysfunction, heart failure, or both. *Circulation* 2010;**122**:597–602.
7. Frangogiannis NG. The extracellular matrix in myocardial injury, repair, and remodeling. *J Clin Invest* 2017;**127**:1600–1612.
8. Lindsey ML, Mann DL, Entman ML, Spinale FG. Extracellular matrix remodeling following myocardial injury. *Ann Med* 2003;**35**:316–326.
9. French BA, Kramer CM. Mechanisms of post-infarct left ventricular remodeling. *Drug Discov Today Dis Mech* 2007;**4**:185–196.
10. de Carvalho LP, Gao F, Chen Q, Hartman M, Sim LL, Koh TH, Foo D, Chin CT, Ong HY, Tong KL, Tan HC, Yeo TC, Yew CK, Richards AM, Peterson ED, Chua T, Chan MY. Differences in late cardiovascular mortality following acute myocardial infarction in three major Asian ethnic groups. *Eur Heart J Acute Cardiovasc Care* 2014;**3**:354–362.
11. Matzinger P. The danger model: a renewed sense of self. *Science* 2002;**296**:301–305.
12. Arslan F, Smeets MB, O'Neill LA, Keogh B, McGuirk P, Timmers L, Tersteeg C, Hoefer IE, Doevendans PA, Pasterkamp G, de Kleijn DP. Myocardial ischemia/reperfusion injury is mediated by leukocytic toll-like receptor-2 and reduced by systemic administration of a novel anti-toll-like receptor-2 antibody. *Circulation* 2010;**121**:80–90.
13. Timmers L, Sluijter JP, van Keulen JK, Hoefer IE, Nederhoff MG, Goumans MJ, Doevendans PA, van Echteld CJ, Joles JA, Quax PH, Piek JJ, Pasterkamp G, de Kleijn DP. Toll-like receptor 4 mediates maladaptive left ventricular remodeling and impairs cardiac function after myocardial infarction. *Circ Res* 2008;**102**:257–264.
14. Arslan F, Smeets MB, Riem Vis PW, Karper JC, Quax PH, Bongartz LG, Peters JH, Hoefer IE, Doevendans PA, Pasterkamp G, de Kleijn DP. Lack of fibronectin-EDA promotes survival and prevents adverse remodeling and heart function deterioration after myocardial infarction. *Circ Res* 2011;**108**:582–592.
15. Blasius AL, Beutler B. Intracellular toll-like receptors. *Immunity* 2010;**32**:305–315.
16. Gao T, Zhang SP, Wang JF, Liu L, Wang Y, Cao ZY, Hu QK, Yuan WJ, Lin L. TLR3 contributes to persistent autophagy and heart failure in mice after myocardial infarction. *J Cell Mol Med* 2018;**22**:395–408.
17. Omiya S, Omori Y, Taneike M, Protti A, Yamaguchi O, Akira S, Shah AM, Nishida K, Otsu K. Toll-like receptor 9 prevents cardiac rupture after myocardial infarction in mice independently of inflammation. *Am J Physiol Heart Circ Physiol* 2016;**311**:H1485–H1497.
18. Celhar T, Hopkins R, Thornhill SI, De Magalhaes R, Hwang SH, Lee HY, Yasuga H, Jones LA, Casco J, Lee B, Thamboo TP, Zhou XJ, Poidinger M, Connolly JE, Wakeland EK, Fairhurst AM. RNA sensing by conventional dendritic cells is central to the development of lupus nephritis. *Proc Natl Acad Sci USA* 2015;**112**:E6195–E6204.
19. Guiducci C, Gong M, Xu Z, Gill M, Chaussabel D, Meeker T, Chan JH, Wright T, Punaro M, Bolland S, Soumelis V, Banchereau J, Coffman RL, Pascual V, Barrat FJ. TLR recognition of self nucleic acids hampers glucocorticoid activity in lupus. *Nature* 2010;**465**:937–941.
20. Christensen SR, Shupe J, Nickerson K, Kashgarian M, Flavell RA, Shlomchik MJ. Toll-like receptor 7 and TLR9 dictate autoantibody specificity and have opposing inflammatory and regulatory roles in a murine model of lupus. *Immunity* 2006;**25**:417–428.
21. Santiago-Raber ML, Dunand-Sauthier I, Wu T, Li QZ, Uematsu S, Akira S, Reith W, Mohan C, Kotzin BL, Izui S. Critical role of TLR7 in the acceleration of systemic lupus erythematosus in TLR9-deficient mice. *J Autoimmun* 2010;**34**:339–348.
22. Zile MR, Mehurg SM, Arroyo JE, Stroud RE, DeSantis SM, Spinale FG. Relationship between the temporal profile of plasma microRNA and left ventricular remodeling in patients after myocardial infarction. *Circ Cardiovasc Genet* 2011;**4**:614–619.
23. Cabrera-Fuentes HA, Ruiz-Meana M, Simsekyilmaz S, Kostin S, Inserte J, Saffarzadeh M, Galuska SP, Vijayan V, Barba I, Barreto G, Fischer S, Lochnit G, Ilinskaya ON, Baumgart-Vogt E, Böning A, Lecour S, Hausenloy DJ, Liehn EA, Garcia-Dorado D, Schlüter K-D, Preissner KT. RNase1 prevents the damaging interplay between extracellular RNA and tumour necrosis factor-alpha in cardiac ischaemia/reperfusion injury. *Thromb Haemost* 2014;**112**:1110–1119.
24. Chen C, Feng Y, Zou L, Wang L, Chen HH, Cai JY, Xu JM, Sosnovik DE, Chao W. Role of extracellular RNA and TLR3-Trif signaling in myocardial ischemia-reperfusion injury. *J Am Heart Assoc* 2014;**3**:e000683.
25. Feng Y, Chen H, Cai J, Zou L, Yan D, Xu G, Li D, Chao W. Cardiac RNA induces inflammatory responses in cardiomyocytes and immune cells via Toll-like receptor 7 signaling. *J Biol Chem* 2015;**290**:26688–26698.
26. Choy MK, Movassagh M, Siggens L, Vujic A, Goddard M, Sanchez A, Perkins N, Figg N, Bennett M, Carroll J, Foo R. High-throughput sequencing identifies STAT3 as the DNA-associated factor for p53-NF-kappaB-complex-dependent gene expression in human heart failure. *Genome Med* 2010;**2**:37.
27. Allijn IE, Czarny BM, Wang X, Chong SY, Weiler M, da Silva AE, Metselaar JM, Lam CS, Pastorin G, de Kleijn DP, Storm G, Wang JW, Schiffelers RM. Liposome encapsulated berberine treatment attenuates cardiac dysfunction after myocardial infarction. *J Control Release* 2017;**247**:127–133.
28. Hu Z, Wang JW, Yu D, Soon JL, de Kleijn DP, Foo R, Liao P, Colecraft HM, Soong TW. Aberrant splicing promotes proteasomal degradation of L-type CaV1.2 calcium channels by competitive binding for CaVbeta subunits in cardiac hypertrophy. *Sci Rep* 2016;**6**:35247.
29. Wang JW, Fontes MSC, Wang X, Chong SY, Kessler EL, Zhang YN, de Haan JJ, Arslan F, Jager Sca D, Timmers L, van Veen TAB, Lam CSP, Kleijn DPV. Leukocytic toll-like receptor 2 deficiency preserves cardiac function and reduces fibrosis in sustained pressure overload. *Sci Rep* 2017;**7**:9193.
30. Ulug U, Goldman S, Ben SI, Shalev E. Matrix metalloproteinase (MMP)-2 and MMP-9 and their inhibitor, TIMP-1, in human term decidua and fetal membranes: the effect of prostaglandin F(2alpha) and indomethacin. *Mol Hum Reprod* 2001;**7**:1187–1193.
31. Heymans S, Luttun A, Nuyens D, Theilmeier G, Creemers E, Moons L, Dyspersin GD, Cleutjens JP, Shipley M, Angellilo A, Levi M, Nube O, Baker A, Keshet E, Lupu F, Herbert JM, Smits JF, Shapiro SD, Baes M, Borgers M, Collen D, Daemen MJ, Carmeliet P. Inhibition of plasminogen activators or matrix metalloproteinases prevents cardiac rupture but impairs therapeutic angiogenesis and causes cardiac failure. *Nat Med* 1999;**5**:1135–1142.
32. Creemers E, Cleutjens J, Smits J, Heymans S, Moons L, Collen D, Daemen M, Carmeliet P. Disruption of the plasminogen gene in mice abolishes wound healing after myocardial infarction. *Am J Pathol* 2000;**156**:1865–1873.
33. Shinde AV, Humeres C, Frangogiannis NG. The role of alpha-smooth muscle actin in fibroblast-mediated matrix contraction and remodeling. *Biochim Biophys Acta Mol Basis Dis* 2017;**1863**:298–309.
34. Fahey TJ, 3rd, Tracey KJ, Tekamp-Olson P, Cousens LS, Jones WG, Shires GT, Cerami A, Sherry B. Macrophage inflammatory protein 1 modulates macrophage function. *J Immunol* 1992;**148**:2764–2769.
35. Bjornadal L, Yin L, Granath F, Klareskog L, Ekbom A. Cardiovascular disease a hazard despite improved prognosis in patients with systemic lupus erythematosus: results from a Swedish population based study 1964-95. *J Rheumatol* 2004;**31**:713–719.
36. McMahon M, Hahn BH, Skaggs BJ. Systemic lupus erythematosus and cardiovascular disease: prediction and potential for therapeutic intervention. *Expert Rev Clin Immunol* 2011;**7**:227–241.
37. Alvarez D, Briassouli P, Clancy RM, Zavadil J, Reed JH, Abellar RG, Halushka M, Fox-Talbot K, Barrat FJ, Buyon JP. A novel role of endothelin-1 in linking Toll-like receptor 7-mediated inflammation to fibrosis in congenital heart block. *J Biol Chem* 2011;**286**:30444–30454.
38. Clancy RM, Alvarez D, Komissarova E, Barrat FJ, Swartz J, Buyon JP. Ro60-associated single-stranded RNA links inflammation with fetal cardiac fibrosis via ligation of TLRs: a novel pathway to autoimmune-associated heart block. *J Immunol* 2010;**184**:2148–2155.
39. Karper JC, Ewing MM, Habets KL, de Vries MR, Peters EA, van Oeveren-Rietdijk AM, de Boer HC, Hamming JF, Kuiper J, Kandimalla ER, La Monica N, Jukema JW, Quax PH. Blocking toll-like receptors 7 and 9 reduces postinterventional remodeling via reduced macrophage activation, foam cell formation, and migration. *Arterioscler Thromb Vasc Biol* 2012;**32**:e72–e80.

40. Liu CL, Santos MM, Fernandes C, Liao M, Iamarene K, Zhang JY, Sukhova GK, Shi GP. Toll-like receptor 7 deficiency protects apolipoprotein E-deficient mice from diet-induced atherosclerosis. *Sci Rep* 2017;**7**:847.
41. Pagni PP, Traub S, Demaria O, Chasson L, Alexopoulou L. Contribution of TLR7 and TLR9 signaling to the susceptibility of MyD88-deficient mice to myocarditis. *Autoimmunity* 2010;**43**:275–287.
42. Cao DJ, Schiattarella GG, Villalobos E, Jiang N, May HI, Li T, Chen ZJ, Gillette TG, Hill JA. Cytosolic DNA sensing promotes macrophage transformation and governs myocardial ischemic injury. *Circulation* 2018;**137**:2613–2634.
43. Matsumura S, Iwanaga S, Mochizuki S, Okamoto H, Ogawa S, Okada Y. Targeted deletion or pharmacological inhibition of MMP-2 prevents cardiac rupture after myocardial infarction in mice. *J Clin Invest* 2005;**115**:599–609.
44. Fang L, Gao XM, Moore XL, Kiriazis H, Su Y, Ming Z, Lim YL, Dart AM, Du XJ. Differences in inflammation, MMP activation and collagen damage account for gender difference in murine cardiac rupture following myocardial infarction. *J Mol Cell Cardiol* 2007;**43**:535–544.
45. Siwik DA, Chang DL, Colucci WS. Interleukin-1beta and tumor necrosis factor-alpha decrease collagen synthesis and increase matrix metalloproteinase activity in cardiac fibroblasts in vitro. *Circ Res* 2000;**86**:1259–1265.
46. Van Linthout S, Miteva K, Tschöpe C. Crosstalk between fibroblasts and inflammatory cells. *Cardiovasc Res* 2014;**102**:258–269.
47. Koulis C, Chen YC, Hausding C, Ahrens I, Kyaw TS, Tay C, Allen T, Jandeleit-Dahm K, Sweet MJ, Akira S, Bobik A, Peter K, Agrotis A. Protective role for Toll-like receptor-9 in the development of atherosclerosis in apolipoprotein E-deficient mice. *Arterioscler Thromb Vasc Biol* 2014;**34**:516–525.
48. Dobaczewski M, Chen W, Frangogiannis NG. Transforming growth factor (TGF)-beta signaling in cardiac remodeling. *J Mol Cell Cardiol* 2011;**51**:600–606.
49. Boyd JH, Mathur S, Wang Y, Bateman RM, Walley KR. Toll-like receptor stimulation in cardiomyoctes decreases contractility and initiates an NF-kappaB dependent inflammatory response. *Cardiovasc Res* 2006;**72**:384–393.
50. Fabbri M, Paone A, Calore F, Galli R, Gaudio E, Santhanam R, Lovat F, Fadda P, Mao C, Nuovo GJ, Zanesi N, Crawford M, Ozer GH, Wernicke D, Alder H, Caligiuri MA, Nana-Sinkam P, Perrotti D, Croce CM. MicroRNAs bind to Toll-like receptors to induce prometastatic inflammatory response. *Proc Natl Acad Sci USA* 2012;**109**:E2110–E2116.
51. Loyer X, Zlatanova I, Devue C, Yin M, Howangyin KY, Klaihmon P, Guerin CL, Kheloufi M, Vilar J, Zannis K, Fleischmann BK, Hwang DW, Park J, Lee H, Menasche P, Silvestre JS, Boulanger CM. Intra-cardiac release of extracellular vesicles shapes inflammation following myocardial infarction. *Circ Res* 2018;**123**:100–106.
52. Chistiakov DA, Orekhov AN, Bobryshev YV. Cardiac extracellular vesicles in normal and infarcted heart. *Int J Mol Sci* 2016;**17**:E63.
53. Sluijter JP, Verhage V, Deddens JC, van den Akker F, Doevendans PA. Microvesicles and exosomes for intracardiac communication. *Cardiovasc Res* 2014;**102**:302–311.